Received: 19 February 2023 | Revised: 6 September 2023 | Accepted: 11 October 2023

DOI: 10.1002/qj.4600

Quarterly Journal of the Royal Meteorological Society RMetS

RESEARCH ARTICLE

On the use of consistent bias corrections to enhance the impact of *Aeolus* Level-2B Rayleigh winds on National Oceanic and Atmospheric Administration global forecast skill

Hui Liu[1,2] | **Kevin Garrett**[3] | **Kayo Ide**[4] | **Ross N. Hoffman**[1,2]

[1]NOAA/NESDIS/Center for Satellite Applications and Research (STAR), College Park, Maryland, USA

[2]Cooperative Institute for Satellite Earth System Studies (CISESS), University of Maryland, College Park, Maryland, USA

[3]NOAA/NWS/Office of Science and Technology Integration (OSTI), Silver Spring, Maryland, USA

[4]University of Maryland, College Park, Maryland, USA

Correspondence
Kevin Garrett, NOAA/NWS/OSTI, 1325 East West Highway, Silver Spring, MD 20910, USA.
Email: kevin.garrett@noaa.gov

Funding information
National Oceanic and Atmospheric Administration, Grant/Award Numbers: NA14NES4320003, NA19NES4320002; NSF, Grant/Award Number: 5234932

Abstract

The operational *Aeolus* Level-2B (L2B) horizontal line-of-sight (HLOS) retrieved Rayleigh winds, produced by the European Space Agency (ESA), utilize European Centre for Medium-Range Weather Forecasts (ECMWF) short-term forecasts of temperature, pressure, and horizontal winds in the Rayleigh–Brillouin and M1 correction procedures. These model fields or backgrounds can contain ECMWF model-specific errors, which may propagate to the retrieved Rayleigh winds. This study examines the sensitivity of the retrieved Rayleigh winds to the changes in the model backgrounds, and the potential benefit of using the same system, in this case the National Oceanic and Atmospheric Administration's Finite-Volume Cubed Sphere Global Forecast System (FV3GFS), for both the corrections and the data assimilation and forecast procedures. It is shown that the differences in the model backgrounds (FV3GFS minus ECMWF) can propagate through the Level-2B horizontal line-of-sight Rayleigh wind retrieval process, mainly the M1 correction, resulting in differences in the retrieved Rayleigh winds with mean and standard deviation of magnitude as large as 0.2 $m \cdot s^{-1}$. The differences reach up to 0.4, 0.6, and 0.7 $m \cdot s^{-1}$ for the 95th, 99th, and 99.5th percentiles of the sample distribution with maxima of ~1.4 $m \cdot s^{-1}$. The numbers of the large differences for the combined lower and upper 5th, 1st, and 0.5th percentile pairs are ~6,100, 1,220, and 610 between 2.5 and 25 km height globally per day respectively. The ESA-disseminated Rayleigh wind product (based on the ECMWF corrections) already shows a significant positive impact on the FV3GFS global forecasts. In the observing system experiments performed, compared with the ESA Rayleigh winds, the use of the FV3GFS-corrected Rayleigh winds lead to ~0.5% more Rayleigh winds assimilated in the lower troposphere and show enhanced positive impact on FV3GFS forecasts at the day 1–10 range but limited to the Southern Hemisphere.

KEYWORDS

Aeolus Rayleigh HLOS winds, M1-temperature-dependent bias correction, NWP impact optimization, Rayleigh–Brillouin correction

1 | INTRODUCTION

Beginning in August 2018, the European Space Agency (ESA) Earth Explorer satellite *Aeolus* has been providing the first observations of wind profiles throughout the troposphere and lower stratosphere from a space-borne Doppler wind lidar (Reitebuch et al., 2020a, 2020b). *Aeolus* measures both Mie and Rayleigh Doppler backscatter from clouds and aerosols and from molecules respectively to derive horizontal line-of-sight (HLOS) Rayleigh and Mie wind profiles (Reitebuch, 2012; Reitebuch et al., 2009; Stoffelen et al., 2005; Straume-Lindner, 2018). In this study, any references to Rayleigh and Mie winds are to *Aeolus* Rayleigh-clear and Mie-cloudy winds respectively. (*Aeolus* Mie winds retrieved under clear conditions and *Aeolus* Rayleigh winds retrieved under cloudy conditions are, to date, of poor quality and are not used in this study.) The Rayleigh observations provide continuous vertical profiles, whereas the Mie observations are few and scattered in the vertical; for example, see Rennie et al. (2021, fig. 1). The *Aeolus* HLOS Level-2B (L2B) Rayleigh and Mie winds have been assimilated in operational data assimilation systems at numerical weather prediction (NWP) centers worldwide and have demonstrated a positive impact on global weather forecasts (e.g., Cress, 2020; Garrett et al., 2022; Pourret et al., 2022; Rennie et al., 2021). The Mie winds are known to be more accurate than the Rayleigh winds; for example, compare figs 2 and 3 of Rennie et al. (2021). However, in general, the more numerous Rayleigh winds show much larger positive impacts on forecast skill (e.g., Liu et al., 2022b).

Information from data assimilation backgrounds (i.e., short-term forecasts) are used to reduce errors in the L2B-retrieved Rayleigh winds in two correction procedures. First, background temperature and pressure are used in the Rayleigh–Brillouin correction (Dabas et al., 2008); second, the background estimates of the Rayleigh HLOS winds are used in the M1 telescope temperature correction (Rennie et al., 2021; Weiler et al., 2021). Operationally, the European Centre for Medium-Range Weather Forecasts (ECMWF) backgrounds are used for these corrections. In the observation system experiments (OSEs) of this study we find a positive impact on the National Oceanic and Atmospheric Administration (NOAA) global forecast when using the NOAA instead of the ECMWF background for these corrections. The anticipation of a positive impact (for reasons given in the next paragraphs) motivated this study.

Informally, we say we do not want to use another model to correct observation biases mainly because of differences in "model climatologies". This is shorthand for the following line of reasoning. In data assimilation, observation and background errors are mixed in the analysis, which are next propagated into the background of the next cycle by the forecast model, which amplifies these errors and adds its own errors. Therefore, the background errors have complex patterns instantaneously and complicated statistics when averaged temporally. These errors and their statistics depend on many factors, including whether it is clear or cloudy, whether it is stormy or not, whether the underlying surface is ocean, land, or ice, and other factors. If one ignores these dependencies then the background errors will appear to be mainly random, but that would be a mistake. The patterns and regularities of the background errors make them difficult to identify and remove. This is the crux of the data assimilation problem. And when we refer to differences in model climatologies we are referring to the collection of differences between the patterns and regularities of the background errors of two different models.

Inevitably, a small part of the model climatology gets into any observation correction method that makes use of information from background fields. When the background comes from a different model than the one assimilating the "corrected" observations, any inconsistencies between the two model climatologies may act in deleterious ways—perturbing the assimilating model state away from its preferred climatology. Thus, the purpose of this study is to see whether eliminating these shocks (plus any associated random differences) to the model system state can have a measurable beneficial impact. In the best linear unbiased estimation paradigm (e.g., Henderson, 1975), which is the foundation of atmospheric data assimilation, to ensure optimal results, the observations should be unbiased relative to the background. It then follows that the observation operator (i.e., the estimator of the observation derived from the background) should not make use of another model's background, which will always include some relative biases. However, replacing the ECMWF backgrounds with some poorer quality NWP model backgrounds would have a deleterious effect on the Rayleigh wind quality. In this study this is not a concern, because the ECMWF and NOAA backgrounds are of comparable quality. But it should be noted that, in the case of a somewhat poorer quality background, the use of consistent corrections might still be sufficient to result in a positive forecast impact due to the advantages described earlier herein.

In this study, the large difference in model climatologies (shown in Figure 1) contain model-dependent components due, for example, to model physics and resolutions. Therefore, using the ECMWF background for the corrections may not be consistent with the Finite-Volume Cubed Sphere Global Forecast System (FV3GFS) model. The differences may propagate and accumulate during the data assimilation cycling, resulting in less optimal

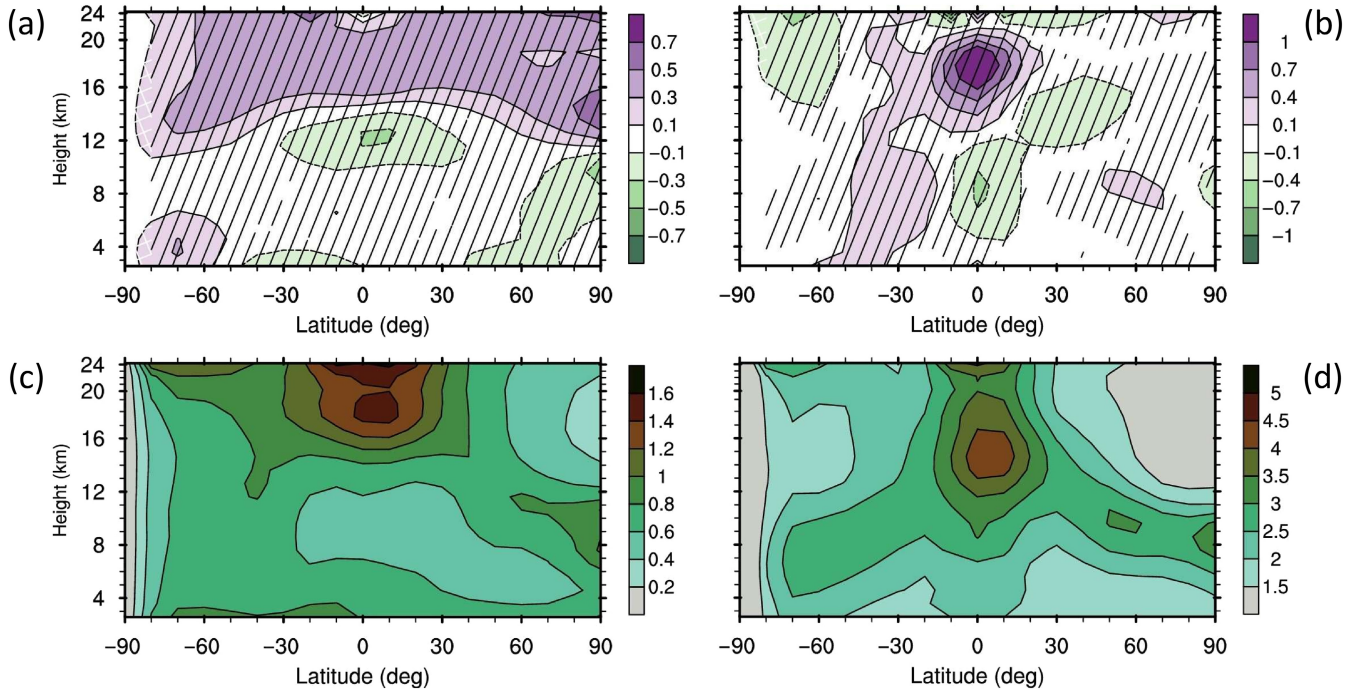

FIGURE 1 Latitude–height cross-sections of the (a, b) mean and (c, d) standard deviation of the background difference (FV3GFS minus ECMWF) for (a, c) temperature (K) and (b, d) horizontal line-of-sight wind ($m \cdot s^{-1}$) at the Rayleigh wind observation locations for ascending orbits for the 6-week study period. Note that the *Aeolus* winds were not assimilated in the operational ECMWF analysis. The hatched areas indicate differences with at least 95% statistical significance. FV3GFS: Finite-Volume Cubed Sphere Global Forecast System; ECMWF: European Centre for Medium-Range Weather Forecasts. [Colour figure can be viewed at wileyonlinelibrary.com]

impacts of the operational Rayleigh winds on FV3GFS analyses and forecasts. Therefore, the assimilation of the Rayleigh wind data in the FV3GFS system might benefit from reproducing the Rayleigh HLOS processing chain for the two corrections but replacing the ECMWF backgrounds with the FV3GFS backgrounds. The hypothesis is that, in this configuration, the Rayleigh winds should contain no influence (neither systematic nor random) from the ECMWF background, should be more consistent with the FV3GFS model, and, therefore, optimize the assimilation of Rayleigh winds in the FV3GFS data assimilation and forecast system.

The purpose of this article is to report the implementation and testing of this configuration; that is, of replacing the ECMWF background by the FV3GFS background in the two corrections. Our tests compare a control (or Base) experiment with two experiments assimilating Rayleigh HLOS winds using, in the first case, the ECMWF operational Rayleigh winds (the RayEC experiment), and in the second case the Rayleigh winds produced using the FV3GFS background in the corrections (the RayGFS experiment). Mie winds are not assimilated in these experiments. The total least-square (TLS) bias correction (Liu et al., 2022a) is applied to the innovations of Rayleigh winds (not to the Rayleigh winds themselves) in these experiments to remove any systematic differences between the Rayleigh winds and FV3GFS background fields that can be described as a simple bias depending on latitude, height, and Rayleigh wind speed. In the present case, the majority of the biases in the Rayleigh winds is removed by the M1 correction. So, the TLS correction is intended mainly to adjust the innovations to effectively ignore the impact of biases in the FV3GFS background, especially in the tropical lower stratosphere. The study (Liu et al., 2022a) shows that the TLS correction improves the impact of ECMWF *Aeolus* winds on FV3GFS forecast.

This study is presented as follows. Section 2 briefly describes the two corrections in the L2B processing, highlighting the use of NWP background fields of temperature, pressure, and HLOS wind. Section 3 discusses differences between the FV3GFS and ECMWF background fields for the study period defined to be 0000 UTC August 2 to September 16, 2019. Section 4 examines the differences in the Rayleigh winds produced by these background differences used in the two corrections. Section 5 describes the parallel OSEs: Base, RayEC, and RayGFS. Then, Section 6 presents the OSE forecast impacts, which demonstrate the benefit on FV3GFS forecast skill of Rayleigh winds corrected using FV3GFS background information in the two corrections. Section 7 presents a summary and conclusions.

Throughout this article, we will use the following terminology. We will refer to *Aeolus* Rayleigh and FV3GFS and ECMWF equivalent HLOS winds as Rayleigh and FV3GFS and ECMWF winds respectively. In addition, Rayleigh winds come in two versions: the FV3GFS-corrected Rayleigh winds and the ECMWF operational Rayleigh winds. In the discussion of winds that are not HLOS winds, we will use terms like *u*-wind, *v*-wind, or wind vector. The term innovation refers to the difference between an observation and an estimate of that observation calculated from the short-term forecast (i.e., the background) of the data assimilation system under consideration. The term bias refers to the mean of a large sample of innovations.

2 | THE USE OF NWP BACKGROUND INFORMATION TO CORRECT RAYLEIGH WIND OBSERVATIONS

There are two main corrections in the ESA/ECMWF operational L2B Rayleigh wind retrieval processing that involve use of ECMWF background fields as a reference that are replicated here but using FV3GFS background fields. A detailed description of the L2B processing is presented by Rennie et al. (2021) and Šavli et al. (2021). Here, we only briefly describe the Rayleigh wind corrections related to the background fields and the modifications used in this study.

First, ECMWF temperature and pressure are used in the Rayleigh-Brillouin correction (Dabas et al., 2008). Without this correction, the *Aeolus* Rayleigh observations could not reach the quality required by NWP users. Estimates based on a standard atmosphere (Dabas et al., 2008) suggest that Rayleigh wind retrieval is sensitive to temperature; and Rayleigh wind error is about a relative error of 0.1% of the true line-of-sight wind for 1 K error in temperature. A typical NWP model background error is a few kelvin. On the other hand, Rayleigh wind retrieval is less sensitive to pressure error, with sensitivities about an order of magnitude smaller for a typical model pressure error of a few hectopascals. Therefore, model errors in the ECMWF background, especially in temperature, will result in an error contribution to the retrieved Rayleigh winds as part of the Rayleigh–Brillouin correction.

Second, Rayleigh wind innovations are used in the M1-temperature-dependent bias correction (hereafter the M1 correction). The small temperature variations across the 1.5 m diameter primary mirror of the telescope (denoted M1) that appear due to variation in radiative effects along the orbit cause errors of up to 8 $m \cdot s^{-1}$ in the Rayleigh winds. The M1 correction is a multiple linear global regression of the Rayleigh wind innovations (from all vertical levels and averaged over 2 min bins, equivalent to 840 km along the track of the wind profiles at the Earth's surface) in terms of predictors defined by measurements of the temperatures at different locations on the M1 mirror (Rennie et al., 2021; Weiler et al., 2021). Note that the M1 correction does not vary in the vertical. The ESA operational "Telescope Correction Suite" software developed by DLR and ECMWF (Weiler et al., 2021) is used for this correction. The regression is updated twice daily using data collected during the previous 24 hr. As a result, errors in ECMWF background winds will have an influence on the Rayleigh winds as part of the M1 correction. As seen in the next sections, the impact of the background differences on Rayleigh winds introduced by the M1 correction is larger than that introduced by the Rayleigh–Brillouin correction.

In this study, the ESA/ECMWF operational L2B Rayleigh winds (version B10) are monitored in the operational FV3GFS-based global four-dimensional ensemble-variational data assimilation system (the Base experiment; see Section 5 for more details). The Base experiment background (3–9 hr hourly forecast) temperature, pressure, and wind are linearly interpolated (from the hourly background at C384, ~25 km resolution and 64 levels) to the Rayleigh wind observation locations and times within the 6 hr assimilation window of each data assimilation cycle and the background equivalent HLOS winds and innovations are calculated. The resulting values are stored in specially formatted AUX_MET files (as described by Šavli et al., 2021) and used in the L2B processor (v3.30) to produce the FV3GFS-corrected Rayleigh winds in this study. With the exception of these FV3GFS AUX_MET files, all the L1B inputs and all the configuration parameters of the L2B processing are identical to those used operationally to produce the L2B10 dataset. The M1 correction for the FV3GFS-corrected Rayleigh winds is determined by the linear regression of the Rayleigh wind innovations of the Base experiment on the M1 mirror temperatures of the previous 24 hr.

3 | NWP BACKGROUND DIFFERENCES

Background winds are interpolated to the locations and times of the L2B Rayleigh wind observations and transformed to equivalent HLOS winds ($HLOS^b$) using

$$HLOS^b = -u^b \sin(\varphi) - v^b \cos(\varphi) \quad (1)$$

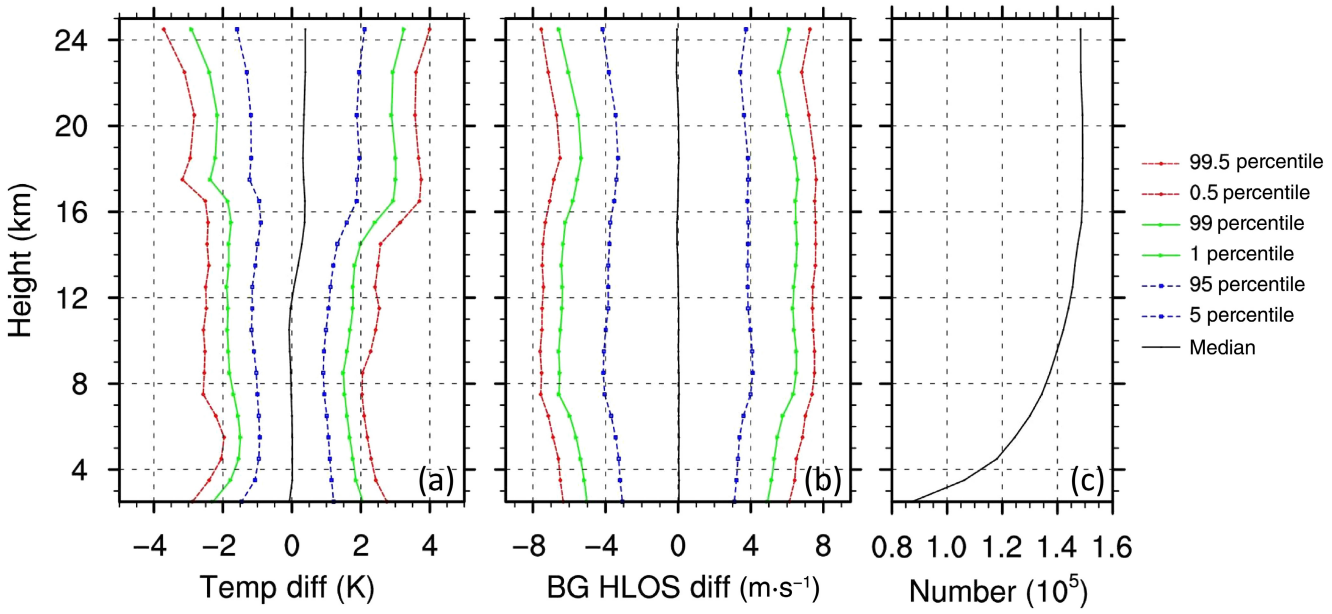

FIGURE 2 The background (a) temperature (K) and (b) HLOS wind ($m \cdot s^{-1}$) difference in the selected sample distribution percentiles (FV3GFS minus ECMWF) at the Rayleigh wind locations for ascending orbits for the 6-week study period. Height bins are 1 km thick from 2 to 19 km and 2 km thick from 19 to 25 km height, and points are plotted at the mean height in each bin. FV3GFS: Finite-Volume Cubed Sphere Global Forecast System; ECMWF: European Centre for Medium-Range Weather Forecasts. [Colour figure can be viewed at wileyonlinelibrary.com]

where b indicates the background, u is the zonal wind component, v is the meridional wind component, and φ is the satellite azimuth angle of the Rayleigh HLOS wind.

Differences between the FV3GFS and ECMWF background fields are due to the combined errors of both and may come from several sources, including the model physics, the model horizontal and vertical resolutions, and how the various observations are used in data assimilation. In Figure 1, the ECMWF background temperatures and winds show noticeable differences to the FV3GFS background values from the Base experiment over regions where conventional observation are sparse, and where model errors are known to be large. Clear differences (FV3GFS minus ECMWF) vary with both latitude and height throughout the troposphere and lower stratosphere. The mean FV3GFS temperature is warmer by up to 0.5 K above 12 km and is somewhat cooler below 12 km. The temperature difference standard deviation is less than 1 K in the mid and high latitudes and reaches a maximum of about 1.6 K in the tropical stratosphere. The HLOS[b] wind differences show a large mean of up to 1.0 $m \cdot s^{-1}$ in the tropical stratosphere and a smaller mean of magnitude 0.5 $m \cdot s^{-1}$ or less almost everywhere else. The difference standard deviation is generally 3 $m \cdot s^{-1}$ or less at the mid and high latitudes and reaches a maximum of about 4.5 $m \cdot s^{-1}$ in the tropical upper troposphere and lower stratosphere.

Figure 2 shows that the differences in the background temperature (FV3GFS minus ECMWF) reach up to 2.0 K, 3.0 K, 4.0 K for the lower and upper 5th, 1st, and 0.5th percentiles of the sample distributions respectively in the lower stratosphere. The difference in the background HLOS winds reach to 4.0 $m \cdot s^{-1}$, 6.0 $m \cdot s^{-1}$, and 7.5 $m \cdot s^{-1}$ for these percentiles respectively.

4 | RAYLEIGH WIND DIFFERENCES DUE TO NWP BACKGROUND DIFFERENCES

First, to estimate the Rayleigh–Brillouin impact of the background temperature and pressure differences on the retrieved Rayleigh winds, we compare the retrieved Rayleigh winds using either FV3GFS or ECMWF temperature and pressure backgrounds before applying the M1 correction (Figure 3). The average differences are, in general, very small except in the lower stratosphere of the Southern Hemisphere, where the mean difference is ~0.04 $m \cdot s^{-1}$ and the standard deviations are about 0.14 $m \cdot s^{-1}$. The differences seem related to the stratosphere polar night jet over the South Pole and the subtropical jet streams—compare with Šavli et al. (2021, fig. 7c)—as well as the large temperature differences there (Figure 1).

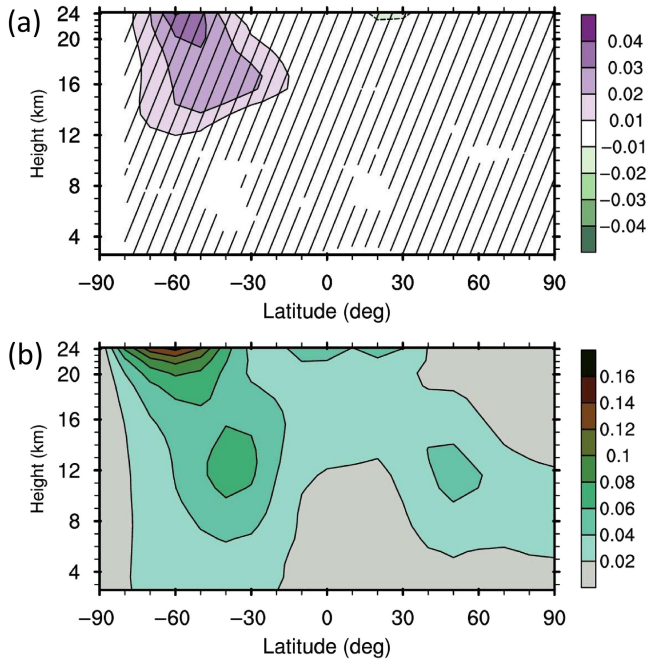

FIGURE 3 Latitude–height cross-sections of the (a) mean and (b) standard deviation of the difference (FV3GFS minus ECMWF) of Rayleigh winds ($m \cdot s^{-1}$) retrieved using the FV3GFS and ECMWF background temperature and pressure fields only (i.e., without the M1 bias correction) for the 6-week study period. The hatched areas indicate differences with at least 95% statistical significance. FV3GFS: Finite-Volume Cubed Sphere Global Forecast System; ECMWF: European Centre for Medium-Range Weather Forecasts. [Colour figure can be viewed at wileyonlinelibrary.com]

The sensitivity of the Rayleigh winds to the temperature differences (FV3GFS minus ECMWF) is estimated by dividing the Rayleigh wind difference (before the M1 correction) by the background temperature difference at each of the Rayleigh wind locations—for a definition, see Šavli et al. (2021, eq. 3). Here, we ignore the negligible impact of the background pressure difference. Figure 4a,c shows the mean and standard deviation of the sensitivity. In general, the sensitivity is much larger in the areas where the Rayleigh wind differences are the largest (comparing Figures 3 and 4). The mean sensitivity and the pattern of the standard deviation of sensitivity are also quite similar to those obtained from the ECMWF operational L2B10 dataset that is calculated analytically from the Rayleigh–Brillouin spectrum (Figure 4b,d).

Including the effect of background wind differences on the M1 correction results in larger differences in the retrieved Rayleigh winds (Figure 5). Figure 5b,d removes from Figure 5a,c the impact of background temperature and pressure differences on the retrieved Rayleigh winds from Figure 3. Comparing the magnitudes of the differences in Figures 3 and 5, the impact of background temperature and pressure differences on the Rayleigh–Brillouin correction is much smaller than the impact of background wind differences on the M1 correction, except in the lower stratosphere of the Southern Hemisphere. As a result, the differences in the retrieved Rayleigh winds (Figure 5) are dominated by the impact of the background wind differences on the M1 correction. The mean difference reaches a value of 0.2 $m\,s^{-1}$, throughout the entire column at 10–20°S. The standard deviation of the differences is at least 0.1 $m\,s^{-1}$ throughout the troposphere and lower stratosphere and reaches 0.2 $m\,s^{-1}$ in the region centered at 60°S. Both the mean and standard deviation of the differences have nearly constant vertical distributions, and especially so in Figure 5b,d. The departure from this pattern around the stratospheric night jet seen in Figure 5c is due to the temperature and pressure impact seen in Figure 3b.

Figure 6 shows the differences in the L2B Rayleigh winds with the M1 correction (FV3GFS minus ECMWF) reach up to 0.4 $m \cdot s^{-1}$, 0.6 $m \cdot s^{-1}$, and 0.7 $m \cdot s^{-1}$ for the 95th, 99th, and 99.5th percentiles of the sample distributions respectively. The differences are a bit smaller in magnitude for the corresponding lower percentiles. The maximum differences are up to 1.4 $m \cdot s^{-1}$, particularly in the Southern Hemisphere (Figure 7). These differences are much larger than the mean and standard deviations of the differences (Figure 5). The number of Rayleigh winds in the combined lower and upper 5th, 1st, and 0.5th percentile pairs are ~6,100, 1,220, and 610 respectively between 2.5 and 25 km height globally per day. These numbers are not negligible compared with current available radiosonde wind observations (~600 profiles globally at 0000 and 1200 UTC).

As will be seen in Section 6, the differences in the Rayleigh winds with M1 correction can lead to large impacts on FV3GFS global forecasts through the cycled assimilation of the Rayleigh winds over the study period.

5 | OSE SETUP

Aeolus L2B Rayleigh and Mie HLOS winds have been integrated and assimilated into the operational FV3GFS global data assimilation and forecast system (Garrett et al., 2022). That system is used in this study. The data assimilation component—the Global Statistical Interpolation (Kleist et al., 2009, 2021)—employs the four-dimensioanl ensemble-variational algorithm with 64 vertical level members (Wang & Lei, 2014). In our experiments, a horizontal resolution denoted C384 (~25 km) is used for the deterministic analysis and forecast. A lower horizontal resolution denoted C192 (~50 km) is used for the ensemble forecasts. The FV3GFS system cycles every 6 hr, and 10-day forecasts are generated from each 0000 UTC analysis.

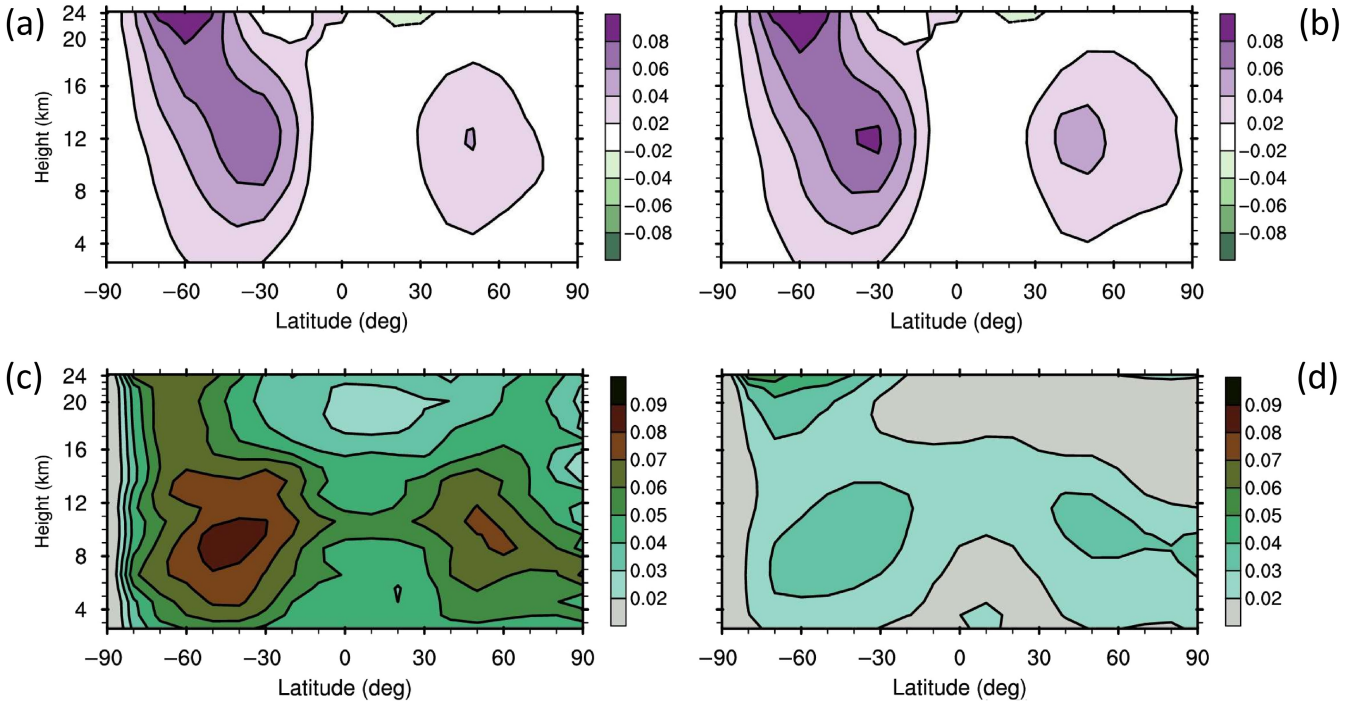

FIGURE 4 Latitude–height cross-sections of the (a, b) mean and (c, d) standard deviation of the sensitivity of Rayleigh winds to temperature ($m \cdot s^{-1} \cdot K^{-1}$). (a, c) Calculated from the ratio of the difference in the (FV3GFS minus ECMWF) retrieved Rayleigh winds without the M1 correction to the difference in the background temperatures for each of the Rayleigh winds. (b, d) Calculated analytically from the Rayleigh–Brillouin spectrum during operational processing with the ECMWF background (and stored in the L2B10 dataset). Otherwise as in Figure 1. FV3GFS: Finite-Volume Cubed Sphere Global Forecast System; ECMWF: European Centre for Medium-Range Weather Forecasts. [Colour figure can be viewed at wileyonlinelibrary.com]

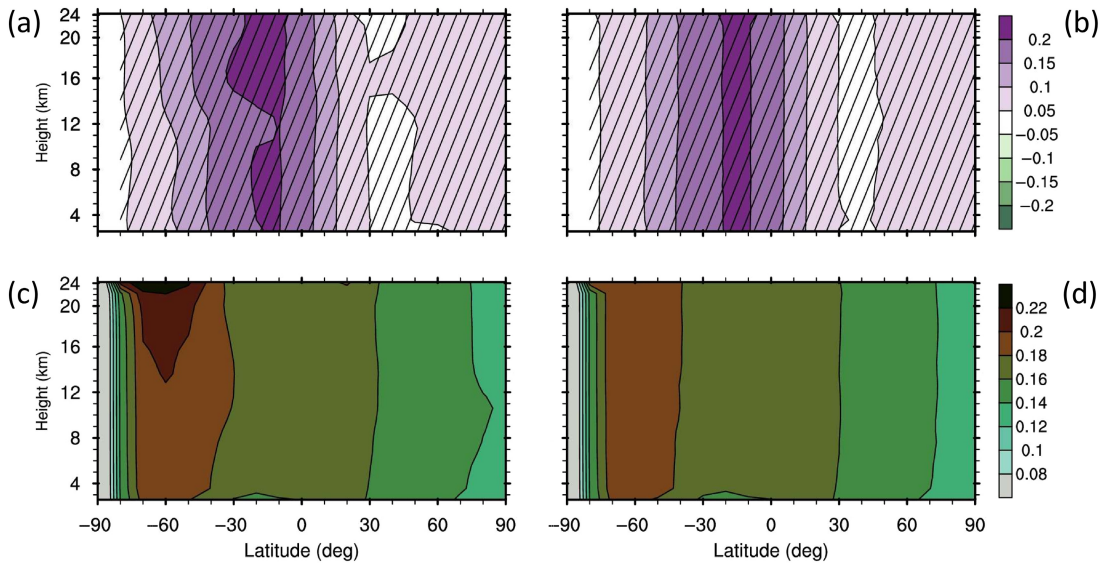

FIGURE 5 Latitude–height cross-sections of the (a) mean and (c) standard deviation of the differences of the (FV3GFS-corrected minus ECMWF operational) Rayleigh winds ($m \cdot s^{-1}$), which include the M1 correction. (b, d) The difference due to the M1 correction alone by removing the mean and variance of the difference due to temperature and pressure corresponding to Figure 3a,b, from (a) and (c) respectively. FV3GFS: Finite-Volume Cubed Sphere Global Forecast System; ECMWF: European Centre for Medium-Range Weather Forecasts. [Colour figure can be viewed at wileyonlinelibrary.com]

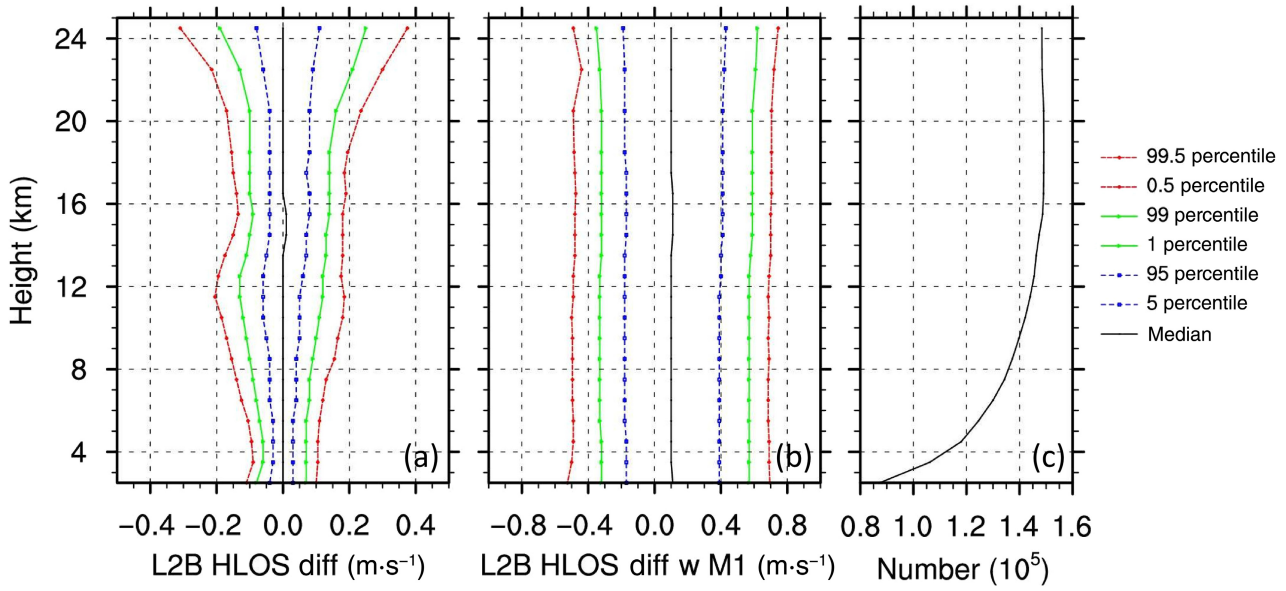

FIGURE 6 The difference in the Level-2B Rayleigh winds (a) without and (b) with the M1 correction (FV3GFS minus ECMWF) in the selected sample distribution percentiles for ascending orbits for the study period. FV3GFS: Finite-Volume Cubed Sphere Global Forecast System; ECMWF: European Centre for Medium-Range Weather Forecasts. [Colour figure can be viewed at wileyonlinelibrary.com]

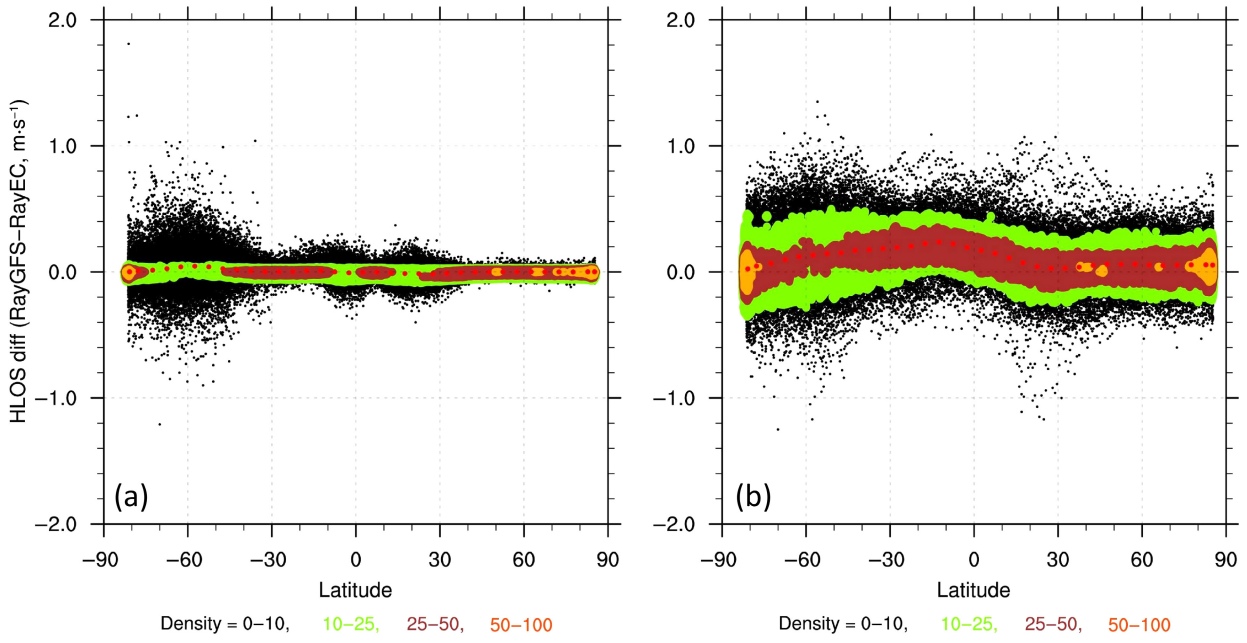

FIGURE 7 Scatterplots of the differences in the Level-2B Rayleigh winds (FV3GFS minus ECMWF) (a) without and (b) with the M1 correction in the 2 km-depth layer centered at 24.5 km for ascending orbits for the study period. FV3GFS: Finite-Volume Cubed Sphere Global Forecast System; ECMWF: European Centre for Medium-Range Weather Forecasts. [Colour figure can be viewed at wileyonlinelibrary.com]

More details of the experimental set-up are given by Garrett et al. (2022).

To assess assimilating the FV3GFS-corrected Rayleigh winds to FV3GFS forecasts, versus assimilating the ECMWF operational Rayleigh winds, two OSEs are performed for the study period in addition to the baseline experiment (Base): the experiment RayEC, which assimilates the ECMWF operational Rayleigh winds; and the parallel experiment RayGFS, which assimilates the FV3GFS-corrected Rayleigh winds. In experiment RayGFS, the FV3GFS-corrected Rayleigh winds are retrieved using the background fields from the Base

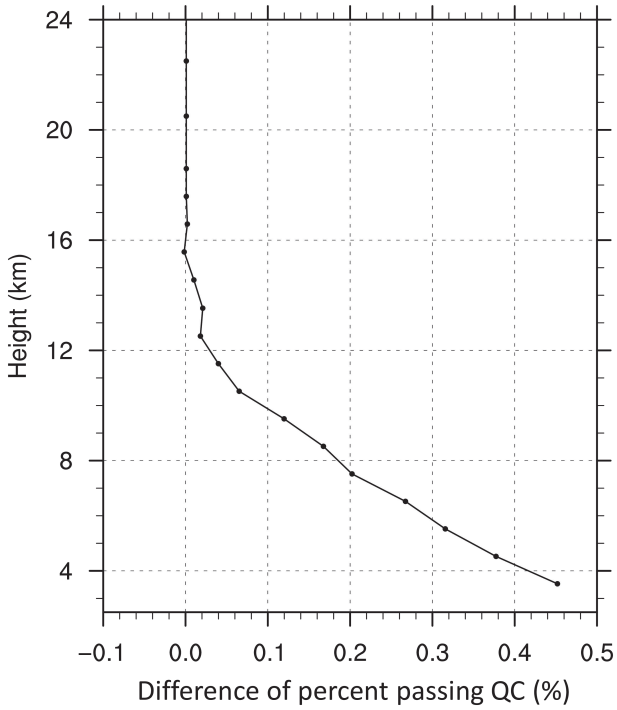

FIGURE 8 The vertical profile of the difference in the percentages of Rayleigh winds that passed the combined European Centre for Medium-Range Weather Forecasts (ECMWF) *Aeolus* and Global Statistical Interpolation quality control tests for the study period in experiments RayEC and RayGFS (RayGFS minus RayEC). RayEC: ECMWF operational Rayleigh winds; RayGFS: Rayleigh winds produced using the Finite-Volume Cubed Sphere Global Forecast System background in the corrections.

experiment as described in Section 2. The experiments begin with the operational FV3GFS analysis valid at 0000 UTC August 2, 2019, and continue data assimilation cycling until 0000 UTC September 16, 2019. The TLS bias correction (Liu et al., 2022a) is applied to the innovations of the Rayleigh winds (not to the Rayleigh winds themselves) in both RayGFS and RayEC experiments, thereby removing a large part of the mean difference due to Rayleigh–Brillouin and M1 corrections in ECMWF operational versus FV3GFS-corrected Rayleigh winds (see Figure 9). As a result, the difference in the impact of Rayleigh winds on the FV3GFS forecast in these experiments should mainly come from the systematic differences in the Rayleigh winds that cannot be described as simple biases depending on latitude, height, and speed, as well as from the random differences in the Rayleigh winds. To isolate the impact due to Rayleigh winds, the Mie winds are not assimilated in the RayGFS and RayEC experiments.

Similar quality control procedures as recommended by the ECMWF (Rennie et al., 2021) are implemented to reject the following Rayleigh winds: winds with L2B confidence flag "invalid"; winds in layers below 850 hPa; winds with L2B estimated errors greater than 12 $m \cdot s^{-1}$; winds with accumulation lengths less than 60 km; and winds at atmospheric pressures within 20 hPa of the topographic surface pressure. A standard outlier check—innovations greater than four times the prescribed Rayleigh wind error—is applied during data assimilation. The percentages of Rayleigh winds that passed all quality control in the RayEC and RayGFS experiments as a function of height are very similar. Figure 8 shows that the difference in this percentage—slightly more Rayleigh winds are assimilated in the lower troposphere in RayGFS, approaching 0.5% of the total in the lowest layer. The assimilation of the additional Rayleigh winds with large innovations could potentially produce a larger impact on forecast skill in RayGFS, compared with RayEC.

Figure 9a shows the mean of the TLS bias correction calculated in the RayEC. There are positive bias corrections with magnitude up to 0.4 $m \cdot s^{-1}$ and negative bias corrections with magnitudes up to 0.6 $m \cdot s^{-1}$ in the lower stratosphere. Larger positive bias corrections with magnitudes up to 0.8 $m \cdot s^{-1}$ exist in the lower troposphere. In RayGFS, the TLS correction differs from RayEC mainly between 0 and 30°S throughout the troposphere and lower stratosphere (Figure 9c), which is consistent with the differences in the Rayleigh winds (Figure 5a). Figure 9c shows a wholesale shift to the negative direction, so the large positive bias corrections in the lower troposphere are reduced due to the use of the FV3GFS Rayleigh winds, but the negative bias corrections become somewhat larger in magnitude. The standard deviations of the TLS bias corrections are similar in the two OSEs.

6 | IMPACTS ON FV3GFS FORECASTS

When evaluating the impact of the Rayleigh wind differences on the OSE experiments, we skip the initial five-day transition period, defining the verification period to include all 161 analyses and all 41 10 day forecasts from 00 UTC 7 August 2019 to 00 UTC 16 September 2019.

The results of the RayEC and RayGFS experiments are evaluated primarily as forecast impacts with respect to the Base experiment, including short-term forecast fits to conventional observations (i.e., statistics of the rawinsonde and aircraft wind observation innovations); forecast vector-wind, temperature, and humidity root-mean-square error (RMSE) time–height cross sections; forecast anomaly correlation "die-off" plots; forecast scorecards; and summary assessment metric (SAM) overall forecast scores. In these results, forecast errors

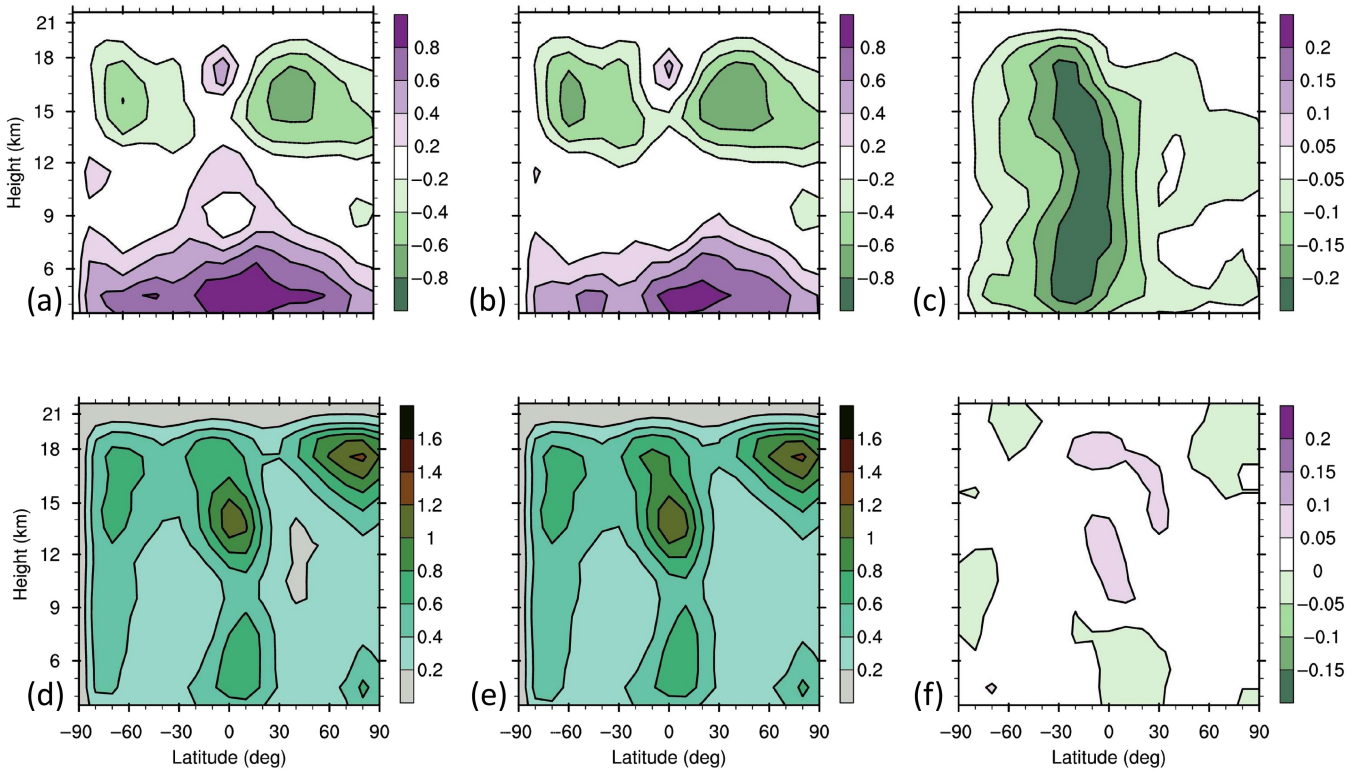

FIGURE 9 Latitude–height cross-sections of the (a, b) mean and (d, e) standard deviation of the total least-square bias correction ($m \cdot s^{-1}$) calculated in the (a, d) RayEC and (b, e) RayGFS experiments for ascending orbits for the 6-week study period. The differences (b) minus (a) and (e) minus (d) are shown in (c) and (f) respectively. RayEC: European Centre for Medium-Range Weather Forecasts operational Rayleigh winds; RayGFS: Rayleigh winds produced using the Finite-Volume Cubed Sphere Global Forecast System background in the corrections. [Colour figure can be viewed at wileyonlinelibrary.com]

are based on verification against the OSEs' self-analyses (instead of ECMWF analysis). This eliminates the impact of ECMWF model climatology through the ECMWF analysis on the verification of the FV3GFS forecasts.

Figure 10 shows the percentage differences relative to the Base experiment of the root-mean-square (RMS) innovations; that is, in the fit of the FV3GFS *u*- and *v*-wind background values to rawinsonde and aircraft wind observations. Note that negative values imply an improvement due to the addition of the Rayleigh winds. Similar improvements in the RMS fits for both RayEC and RayGFS experiments are seen in Figure 10a–f, with no impacts in the Northern Hemisphere. The largest improvement is a 3–4% reduction relative to the Base RMS that occurs for the *u*-wind above 200 hPa in the Tropics. The improvements in the Southern Hemisphere for both the *u*- and *v*-wind, as well as in the Tropics for the *v*-wind, are smaller, typically 1% throughout the troposphere. In general, the differences between RayEC and RayGFS experiments are negligible.

The impact of Rayleigh wind differences on the 10-day FV3GFS global forecast is much greater in the Southern Hemisphere. Cross-sections of the vector-wind, temperature, and relative humidity forecast RMSE from 50 to 1,000 hPa for forecast days 1–10 in Base, verified against the OSEs' self-analyses, for the Southern Hemisphere are shown in Figure 11a–c. The differences in forecast RMSE between RayEC and Base and between RayGFS and Base as a percentage of the Base RMSE are shown in the Figure 11d–f and g–i respectively. In general, there are clear improvements in forecast skill due to the addition of the Rayleigh winds. The improvements are typically greater and statistically significant in the upper troposphere and lower stratosphere. For forecast days 1–3, the improvements in RayEC and RayGFS are similar in the lower stratosphere and upper troposphere. But forecast skill improvement in RayGFS is clearer and larger in the lower troposphere, particularly in temperature compared with in RayEC. For forecasts after day 3, the RayEC impacts decay, lose their statistical significance, and eventually become slightly negative, whereas the RayGFS impacts continue to be positive and statistically significant, increasingly so for vector wind and temperature.

Considering the wind impacts for RayEC, the largest error reduction (−3.5%) occurs at 0–80 hr lead times. Some minor degradation is seen at forecast lead times >200 hr.

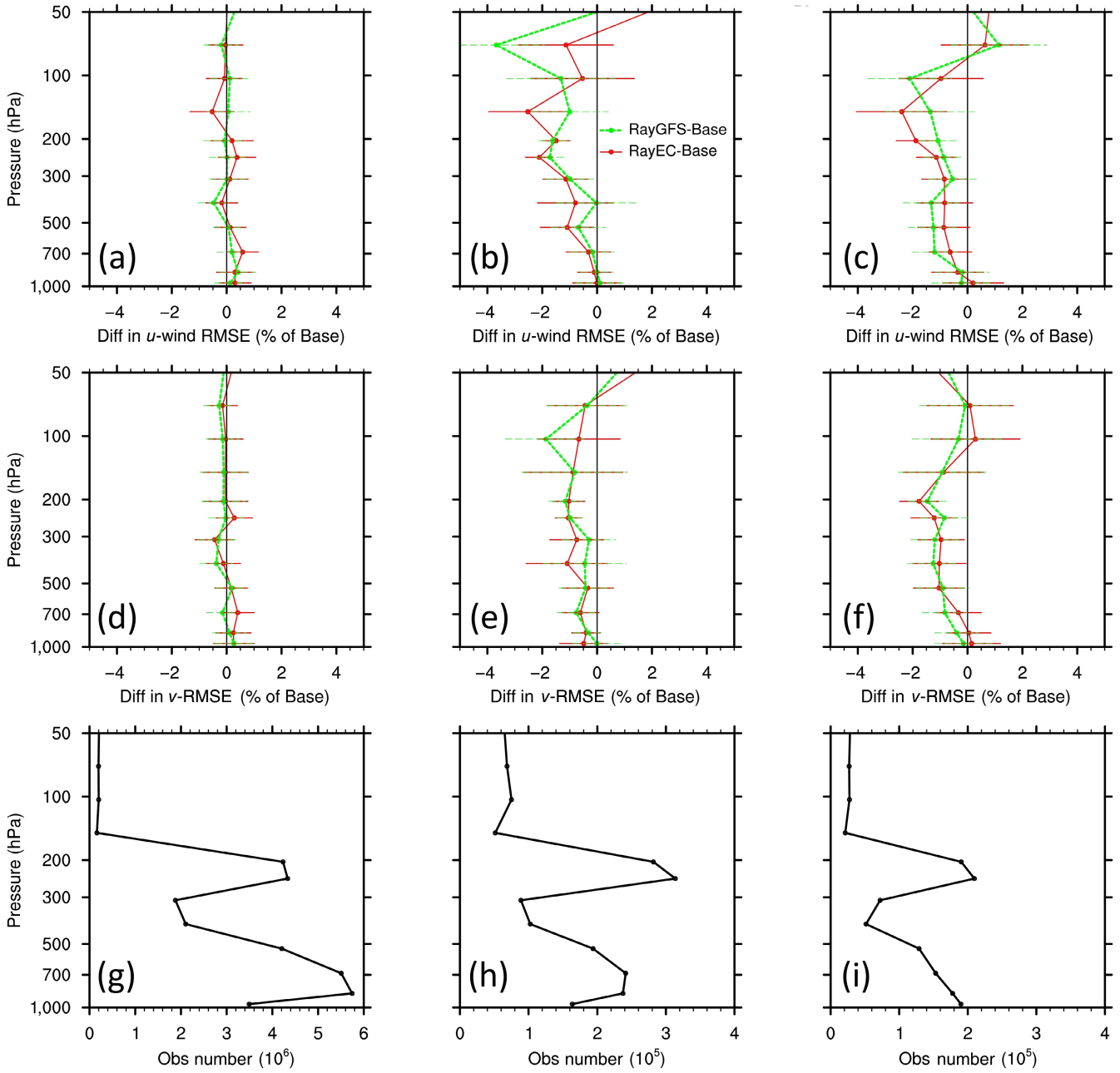

FIGURE 10 Profiles of the percent differences relative to the Base experiment of the root-mean-square wind-component innovations, for RayEC minus Base (red lines) and RayGFS minus Base (green lines) for rawinsonde and aircraft (a–c) *u*-wind and (d–f) *v*-wind in the (a, d) Northern Hemisphere, (b, e) Tropics, and (c, f) Southern Hemisphere. Horizontal bars denote the 95% confidence in each layer. (g)–(i) The numbers of rawinsonde and aircraft wind observations used in the statistics. RayEC: European Centre for Medium-Range Weather Forecasts operational Rayleigh winds; RayGFS: Rayleigh winds produced using the Finite-Volume Cubed Sphere Global Forecast System background in the corrections. [Colour figure can be viewed at wileyonlinelibrary.com]

In RayGFS, the vector-wind RMSE is reduced at all forecast lead times. A large part of the improvement is statistically significant at the 95% significance level. The impact on temperature forecast RMSE is positive at forecast lead times <120 hr in RayEC, with the largest error reduction (2–3%). Some minor degradation is seen at forecast lead times >120 hr. In RayGFS, the temperature forecast RMSE is reduced more at all forecast lead times, particularly in the lower troposphere.

For relative humidity, the forecast RMSE in RayEC is reduced by up to ~4% above 200 hPa at most forecast lead times, and ~0.5% in the troposphere at lead times <80 hr. In RayGFS, the RMSE reduction is considerably larger at all lead times. It should also be noted, however, that there

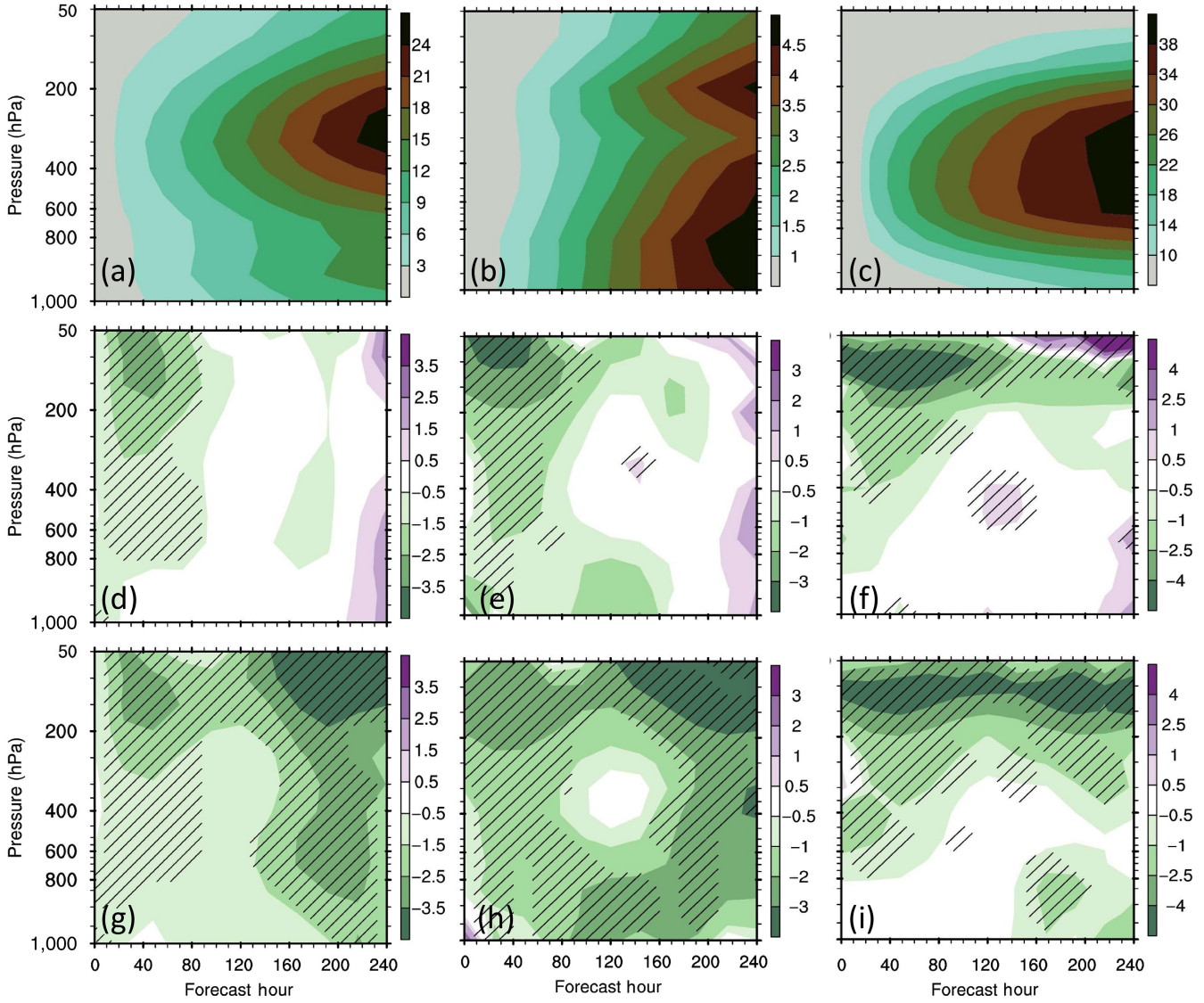

FIGURE 11 Southern Hemisphere forecast statistics in time versus pressure cross-sections of (a, d, g) vector-wind, (b, e, h) temperature, and (c, f, i) relative humidity. (a)–(c) The forecast root-mean-square error (RMSE) in the Base experiment with units of $m \cdot s^{-1}$, K, and % respectively. (d)–(i) The differences in the forecast RMSE with respect to Base (%) for (d–f) the RayEC experiment and (g–i) the RayGFS experiment. The hatched areas indicate changes with at least 95% statistical significance. RayEC: European Centre for Medium-Range Weather Forecasts operational Rayleigh winds; RayGFS: Rayleigh winds produced using the Finite-Volume Cubed Sphere Global Forecast System background in the corrections. [Colour figure can be viewed at wileyonlinelibrary.com]

remains high uncertainty in the analysis of humidity in that region due to many factors, including the low volume of humidity observations and their higher uncertainty due to the overall low absolute humidity.

In the Northern Hemisphere, the ECMWF Rayleigh winds in general show a neutral impact on forecast skills at lead times <160 hr and a degradation at lead times >160 hr in RayEC (Figure 12). The FV3GFS-corrected Rayleigh winds turn the degradation to improvement. In the Tropics, both ECMWF and FV3GFS-corrected Rayleigh winds show similar positive impact on forecast skills at all lead times in RayEC and RayGFS (Figure 13).

The 500 hPa height anomaly correlation (AC) for RayGFS shows a statistically significant improvement for the days 5–9 forecast in the Southern Hemisphere compared with the RayEC (Figure 14b,d). The AC decays to 0.60 at hour 204 for RayEC compared with hour 214 for RayGFS. The impact of Rayleigh winds in the Northern Hemisphere is neutral for RayGFS and slightly negative (but not statistically significant) for RayEC (Figure 14a,c).

The National Centers for Environmental Prediction forecast skill scorecards for RayEC and RayGFS versus Base (Figure 15) provide a comprehensive evaluation of the global forecast skill out to 10 days in terms of RMSE

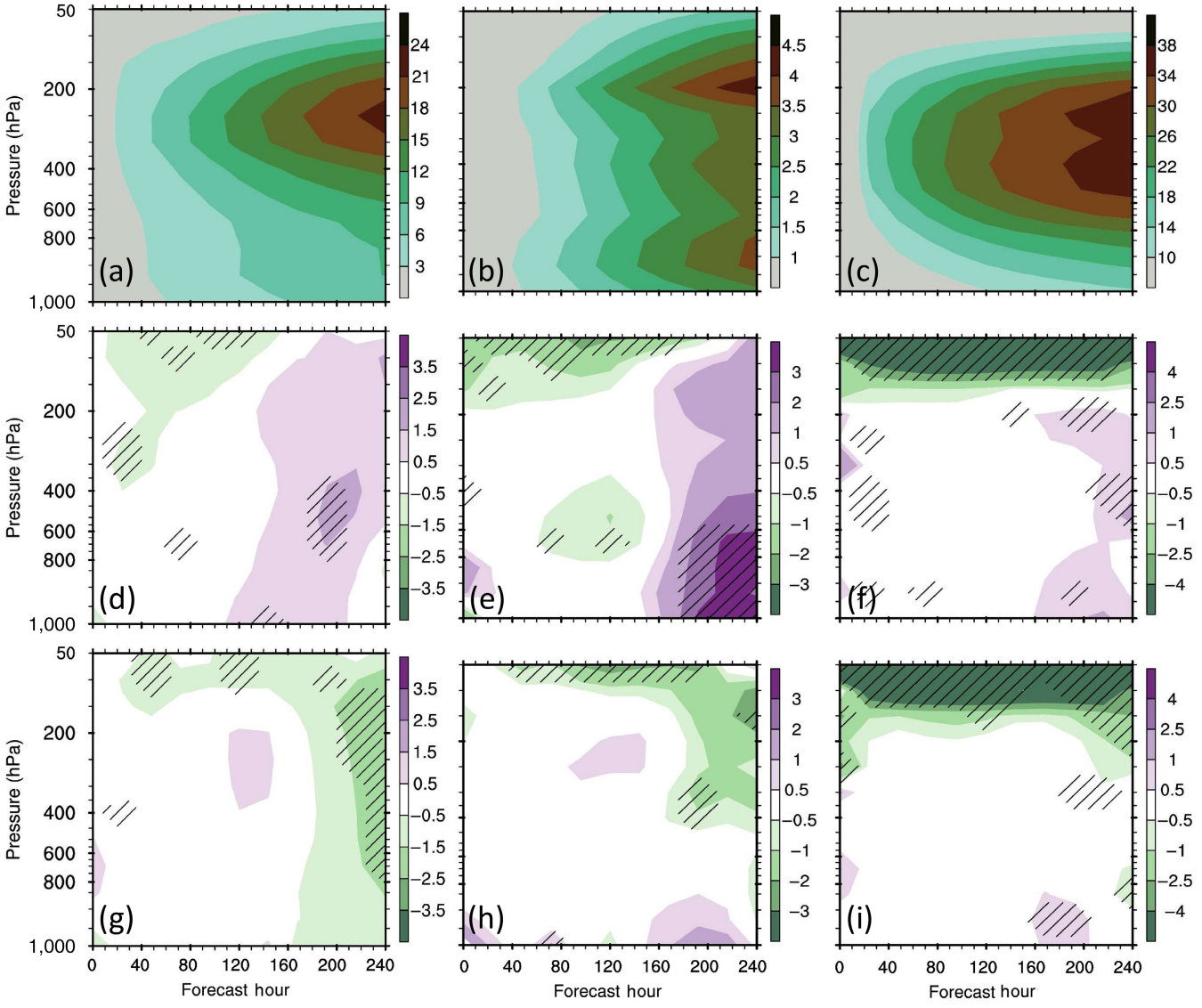

FIGURE 12 The same as Figure 11, but for in the Northern Hemisphere. [Colour figure can be viewed at wileyonlinelibrary.com]

and AC. The Rayleigh winds have statistically significant positive impacts on forecast skill for vector-wind and temperature in the Southern Hemisphere and in the Tropics in RayEC for days 1–3, but neutral impacts in the Northern Hemisphere. In RayGFS, the assimilation of the FV3GFS-corrected Rayleigh winds leads to further improvement on forecast skill for days 1–10 in the Southern Hemisphere. The forecast skills in RayEC and RayGFS for days 1–10 are, in general, similar in the Northern Hemisphere and in the Tropics.

To quantify the aforementioned results overall, SAMs are computed for the RayEC and RayGFS experiments relative to the Base experiment. The SAMs illustrates the overall forecast skill by normalizing diverse statistics and computing an empirical cumulative density function (Hoffman et al., 2018). Figure 16 shows the SAM difference scores for RayEC and RayGFS experiments with respect to the Base experiment. In addition to the overall SAM scores, the SAM scores are shown separately for forecast lead times in the Northern Hemisphere, Tropics, and Southern Hemisphere. The ECMWF operational Rayleigh winds in general have a positive impact on the forecast days 1–3 in the Southern Hemisphere and on forecast days 1–10 in the Tropics. Significant forecast skill enhancement is seen in forecast days 3–10 in the Southern Hemisphere in the RayGFS experiment. In the Tropics, the impact of the Rayleigh winds on forecast skills is similar in RayEC and RayGFS. In the Northern Hemisphere, the ECMWF Rayleigh winds show a neutral impact, except for a negative impact on forecast days 8–10. The FV3GFS-corrected Rayleigh winds reverse the negative impact to a positive impact. The overall improvement by Rayleigh winds for RayEC and RayGFS experiments is about 2% and 5% respectively, illustrating the enhanced forecast skill with the FV3GFS-corrected Rayleigh winds.

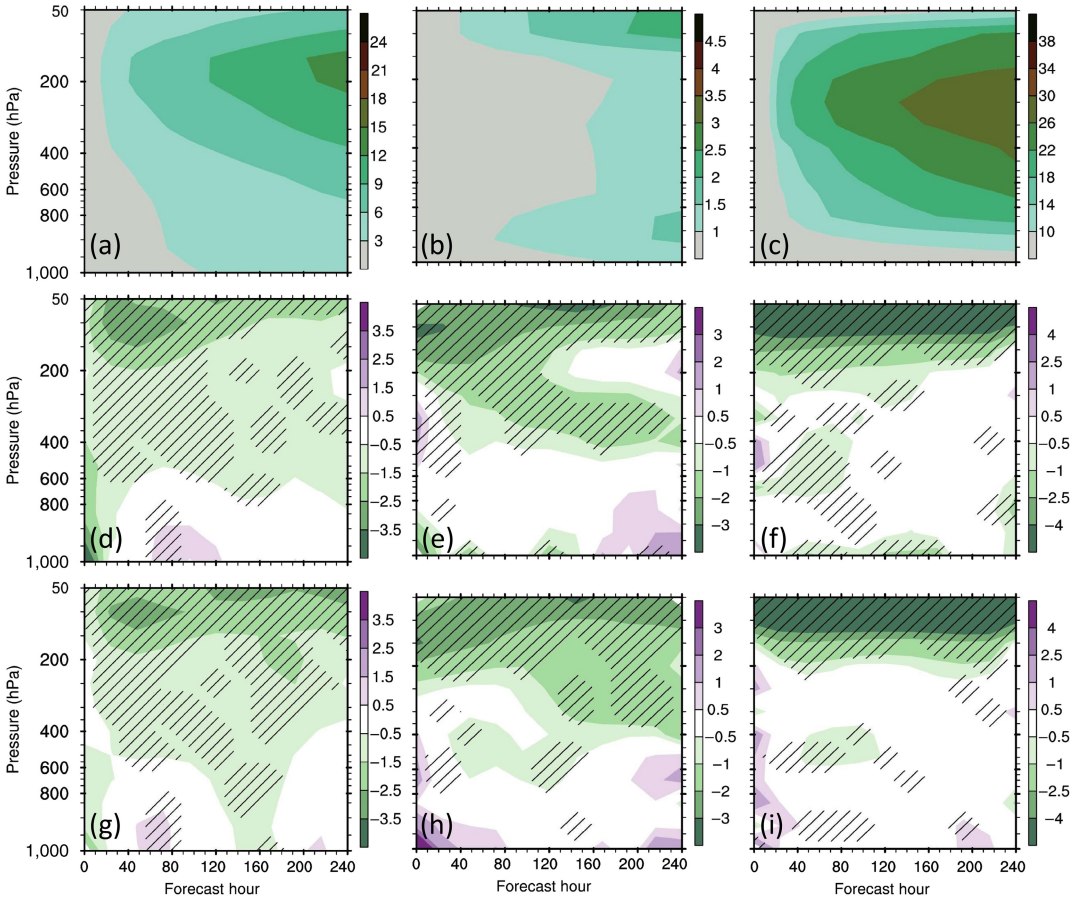

FIGURE 13 The same as Figure 11, but for in the Tropics. [Colour figure can be viewed at wileyonlinelibrary.com]

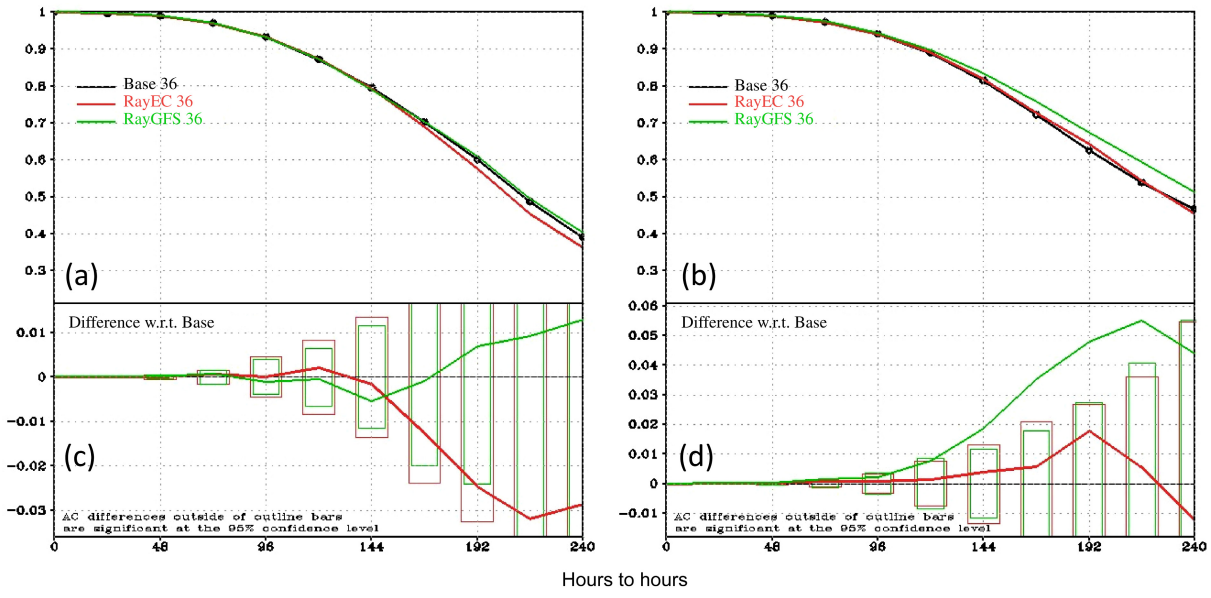

FIGURE 14 (a), (b) Anomaly correlation (AC) of Finite-Volume Cubed Sphere Global Forecast System (FV3GFS) 500 hPa height 0–10 day forecasts (verified against the observation system experiments' self-analyses) in the Base, RayEC, and RayGFS experiments for (a, c) Northern Hemisphere and (b, d) Southern Hemisphere. (c), (d) The differences in the ACs of RayEC and RayGFS versus Base, with bars representing the 95% confidence interval. RayEC: European Centre for Medium-Range Weather Forecasts operational Rayleigh winds; RayGFS: Rayleigh winds produced using the FV3GFS background in the corrections. [Colour figure can be viewed at wileyonlinelibrary.com]

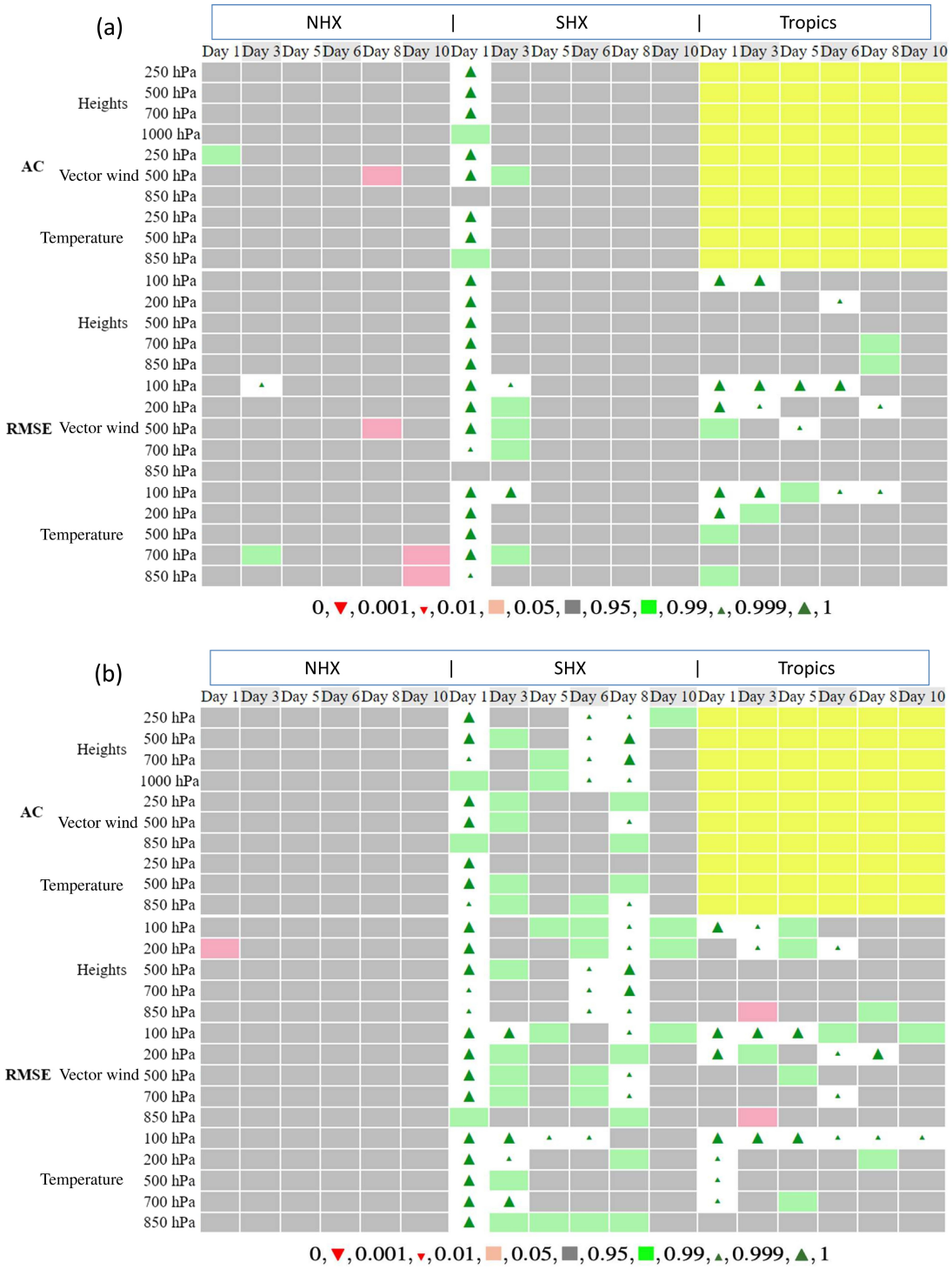

FIGURE 15 Finite-Volume Cubed Sphere Global Forecast System (FV3GFS; 1–10 days) forecast skill scorecard comparing (a) RayEC versus Base and (b) RayGFS versus Base. Note that only anomaly correlation (AC) and root-mean-square (RMSE) heights, winds, and temperatures for the Northern Hemisphere extratropics (NHX), Southern Hemisphere extratropics (SHX), and Tropics are extracted to create this figure. The symbols and colors indicate the probability that an experiment is better than Base. As shown below the scorecard, the green symbols (from left to right) indicate that an experiment is better than Base at the 95%, 99%, and 99.9% significance levels respectively, whereas the red symbols indicate that an experiment is worse than Base at the 99.9%, 99%, and 95% significance levels respectively. Gray indicates no statistically significant differences. RayEC: European Centre for Medium-Range Weather Forecasts operational Rayleigh winds; RayGFS: Rayleigh winds produced using the FV3GFS background in the corrections. [Colour figure can be viewed at wileyonlinelibrary.com]

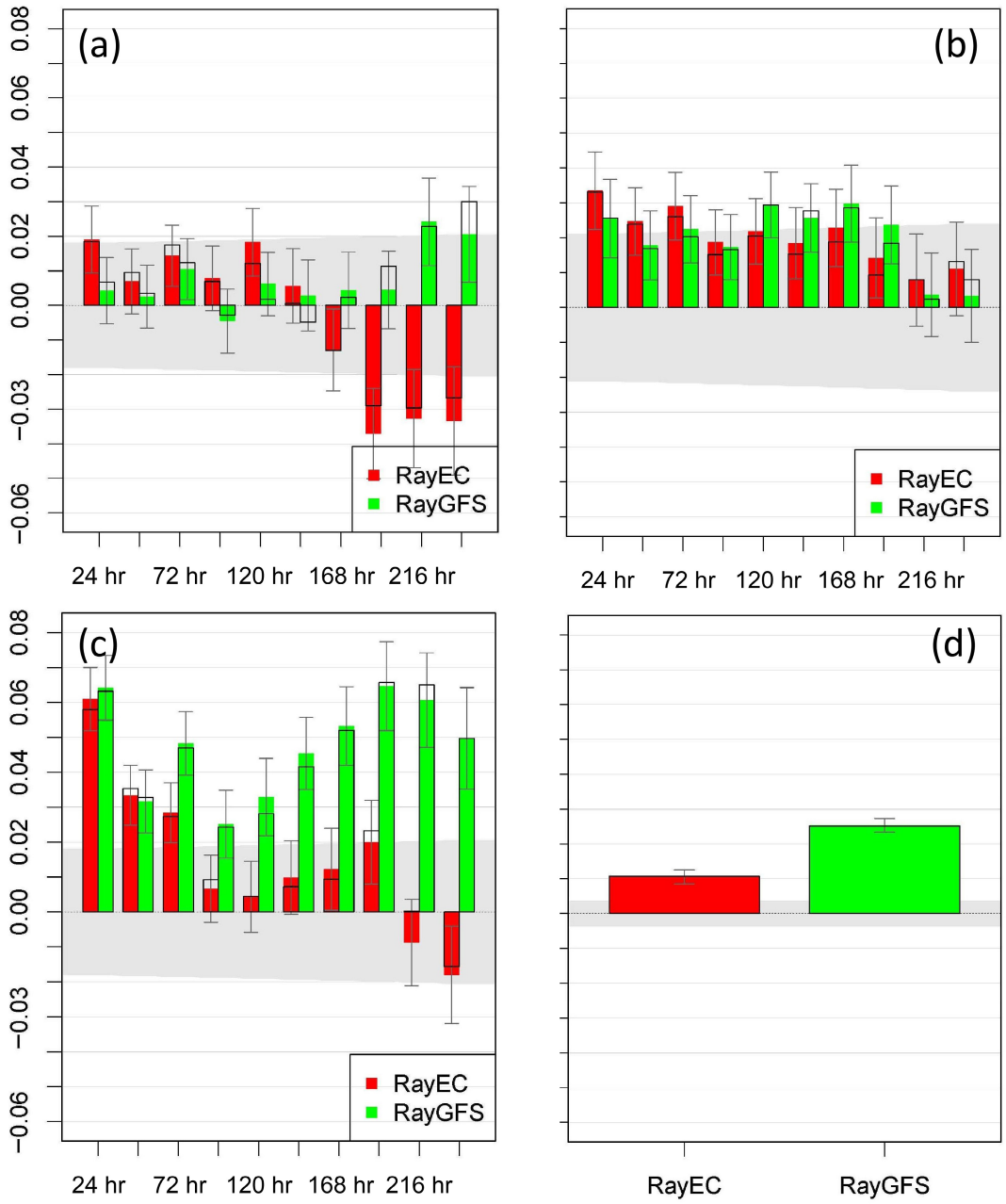

FIGURE 16 The difference summary assessment metrics (SAMs) for RayEC and RayGFS versus Base experiments. The SAMs are shown for 1–10 days forecast lead times in the (a) Northern Hemisphere extratropics, (b) Tropics, (c) Southern Hemisphere extratropics, and (d) for overall performance. The gray areas indicate the 95% confidence interval under the null hypothesis that there is no difference between experiments for this metric. In addition, the estimated uncertainty at the 95% level is indicated by small error bars at the ends of the color bars. Two normalizations are used, the empirical cumulative density function (color-shaded) and rescaled-minmax normalization (black outline). Values above 0.0 represent an improvement of the forecast versus the Base. A value of 0.02, for example, indicates the average normalized statistic is better (greater) by 0.02 than Base. Under the null hypothesis that there are no differences, all SAMs would be 0.5, so a 0.02 improvement can be considered a 4% improvement in normalized scores. Details are in Hoffman et al. (2018). RayEC: European Centre for Medium-Range Weather Forecasts operational Rayleigh winds; RayGFS: Rayleigh winds produced using the Finite-Volume Cubed Sphere Global Forecast System background in the corrections. [Colour figure can be viewed at wileyonlinelibrary.com]

The aforementioned results show that the FV3GFS forecast of RayEC shows improvement in skill for days 1–3 only in the Southern Hemisphere, whereas the FV3GFS forecast of RayGFS shows statistically significant enhanced improvements in skill for days 1–10. The forecast skills of RayEC and RayGFS are, in general, similar in the Northern Hemisphere and in the Tropics.

7 | SUMMARY AND CONCLUSIONS

In this study, we examine the benefit to NOAA global forecasts when the *Aeolus* Level-2B Rayleigh winds are prepared using FV3GFS background temperature, pressure, and winds in place of the corresponding ECMWF background fields in the Rayleigh–Brillouin correction and the M1-temperature-dependent bias correction.

The differences in temperature and HLOS wind between FV3GFS and ECMWF backgrounds evaluated at the Rayleigh wind observation locations and times for the study period of August 2–September 16, 2019, are largest in the Southern Hemisphere and Tropics, with largest maxima in the tropical lower stratosphere. Specifically, the temperature background mean and standard deviation of the differences range up to 0.5 K and 1.6 K respectively. The background HLOS winds have mean differences up to 1.0 $m \cdot s^{-1}$ and standard deviation differences up to 3.0 $m \cdot s^{-1}$ in the mid to high latitudes and up to 4.0 $m \cdot s^{-1}$ in the Tropics. The differences for the 99.5th percentile reach ~4 K and 7.5 $m \cdot s^{-1}$ for background temperature and HLOS winds respectively.

These background field differences can have impact on the Rayleigh–Brillouin correction, and particularly the M1 correction, and result in small (about 0.2 $m \cdot s^{-1}$) mean and standard deviation of the differences in the retrieved Rayleigh winds, mainly near the stratospheric night jet and the subtropical jet in the Southern Hemisphere. The Rayleigh wind differences due to the Rayleigh–Brillouin and mainly M1 correction reach up to 0.4 $m \cdot s^{-1}$, 0.6 $m \cdot s^{-1}$, and 0.7 $m \cdot s^{-1}$ for the 95th, 99th, and 99.5th percentiles of the sample distribution respectively, with maximum magnitude of ~1.4 $m \cdot s^{-1}$. The number of Rayleigh winds in the combined lower and upper 5th, 1st, and 0.5th percentile pairs are ~6,100, 1,220, and 610 respectively between 2.5 and 25 km height globally per day. These numbers are not negligible considering current available radiosonde wind observations (~600 profiles globally at 0000 and 1200 UTC). The use of FV3GFS-corrected Rayleigh winds also affects quality control, leading to ~0.5% more Rayleigh winds assimilated in the lower troposphere. In the OSEs performed, the impact of the differences in the Rayleigh winds results in neutral impacts on the innovations of radiosonde and aircraft wind observations but leads to large differences in the FV3GFS 10-day forecasts in the Southern Hemisphere. Considerably enhanced positive impacts of the FV3GFS-corrected Rayleigh winds on forecasts compared with those of the ECMWF operational Rayleigh winds are seen in the Southern Hemisphere at the days 1–10 range.

One of potential reasons for the large differences in impact of Rayleigh winds on the days 4–10 forecast skill of RayEC and RayGFS in the Southern Hemisphere might be related to predictability associated with the regional atmospheric structures, like the strong lower stratospheric jet, where the ECMWF and FV3GFS model backgrounds show large differences—see Šavli et al. (2021, fig. 1, cf. fig. 7c). Further study is needed to understand this.

Taken together, the results show substantial benefit to the NOAA Global Forecast System of using its own background in the two corrections of L2B Rayleigh wind processing. The results might suggest that it would be beneficial for other NWP centers to perform the Rayleigh wind corrections, particularly the M1 correction, using their own model backgrounds, but such a benefit would depend on the quality of those backgrounds.

ACKNOWLEDGEMENTS

This work was supported by the NOAA/NESDIS Office of Projects, Planning, and Acquisition (OPPA) Technology Maturation Program (TMP) through CICS/CISESS at the University of Maryland (NA14NES4320003 and NA19NES4320002) managed by Patricia Weir and Dr Nai-Yu Wang, as well as NSF grant 5234932. We acknowledge Michael Rennie (ECMWF) for providing useful comments on the assimilation of *Aeolus* observations, Dr William McCarty (NASA/GMAO) for providing earlier versions of the Global Statistical Interpolation with *Aeolus* ingest and observation operator capability, and Dr Jos de Kloe (KNMI) for helping with the *Aeolus* L2B processing. The *Aeolus* L1B/L2B data were provided by the ESA. The scientific results and conclusions, as well as any views or opinions expressed herein, are those of the authors and do not necessarily reflect those of NOAA or the US Department of Commerce.

DATA AVAILABILITY STATEMENT

The *Aeolus* L2B Earth Explorer data used in this study are publicly available and can be accessed via the ESA Aeolus Online Dissemination System (https://aeolus-ds.eo.esa.int/oads/access/). The data related to the *Aeolus* assimilation experiment outputs are not publicly available due to the huge volume of data. We will try to provide access to the data upon request.

ORCID

Hui Liu https://orcid.org/0000-0002-7959-0984
Kevin Garrett https://orcid.org/0000-0002-7444-4363

Kayo Ide https://orcid.org/0000-0001-5789-9326
Ross N. Hoffman https://orcid.org/0000-0002-4962-9438

REFERENCES

Cress, A. (2020) 'Validation and impact assessment of Aeolus observations in the DWD modeling system. Status report'. *Aeolus NWP Impacts Working Meeting*, Virtual. Available from: https://www.aeolus3years.org/detailed-agenda [Accessed 15 November 2020]

Dabas, A., Denneulin, M.L., Flamant, P., Loth, C., Garnier, A. & Dolfi-Bouteyre, A. (2008) Correcting winds measured with a Rayleigh Doppler lidar from pressure and temperature effects. *Tellus A*, 60, 206–215. Available from: https://doi.org/10.1111/j.1600-0870.2007.00284.x

Garrett, K., Liu, H., Ide, K., Hoffman, R.N. & Lukens, K.E. (2022) Optimization and impact assessment of Aeolus HLOS wind data assimilation in NOAA's global forecast system. *Quarterly Journal of the Royal Meteorological Society*, 148, 2703–2716. Available from: https://doi.org/10.1002/qj.4331

Henderson, C.R. (1975) Best linear unbiased estimation and prediction under a selection model. *Biometrics*, 31(2), 423–447. Available from: https://doi.org/10.2307/2529430

Hoffman, R.N., Kumar, K., Boukabara, S., Yang, F. & Atlas, R. (2018) Progress in forecast skill at three leading global operational NWP centers during 2015–17 as seen in summary assessment metrics (SAMs). *Weather and Forecasting*, 33, 1661–1679. Available from: https://doi.org/10.1175/WAF-D-18-0117.1

Kleist, D.T., Parrish, D.F., Derber, J.C., Treadon, R., Wu, W.S. & Lord, S. (2009) Introduction of the GSI into the NCEP global data assimilation system. *Weather Forecasting*, 24, 1691–1705. Available from: https://doi.org/10.1175/2009WAF2222201.1

Kleist, D.T., Treadon, R., Thomas, C., Liu, H., Bathmann, K., Merkova, D. et al. (2021) NCEP operational global data assimilation upgrades: from versions 15 through 16. In101st American Meteorological Society Annual Meeting. Available from: https://ams.confex.com/ams/101ANNUAL/meetingapp.cgi/Paper/378554

Liu, H., Garrett, K., Ide, K., Hoffman, R.N. & Lukens, K. (2022b) *'A comprehensive assessment of Aeolus wind impact on NOAA global forecast', ESA 3rd Aeolus conference, 28 March–1 April 2022*. Italy: Taormina. Available from: https://www.aeolus3years.org/detailed-agenda

Liu, H., Garrett, K., Ide, K., Hoffman, R.N. & Lukens, K.E. (2022a) A statistically optimal analysis of systematic differences in winds from Aeolus level-2B data and the NOAA/FV3GFS. *Atmospheric Measurement Techniques*, 15, 3925–3940. Available from: https://doi.org/10.5194/amt-2022-20

Pourret, V., Šavli, M., Mahfouf, J.F., Raspaud, D., Doerenbecher, A., Bénichou, H. et al. (2022) Operational assimilation of Aeolus winds in the Météo-France global NWP model ARPEGE. *Quarterly Journal of the Royal Meteorological Society*, 148(747), 2652–2671.

Reitebuch, O. (2012) The Spaceborne wind Lidar Mission ADM-Aeolus. In: Schumann, U. (Ed.) *Atmospheric physics. Research topics in aerospace*. Berlin, Heidelberg: Springer, pp. 815–827.

Reitebuch, O., Krisch, I., Lemmerz, C., Lux, O., Marksteiner, U., Masoumzadeh, N. et al. (2020b) 'Assessment of Aeolus performance and bias correction- results from the Aeolus DISC'. Aeolus Cal/Val and Science Workshop 2020. https://nikal.eventsair.com/QuickEventWebsitePortal/2ndaeolus-post-launch-calval-and-science-workshop/aeolus

Reitebuch, O., Lemmerz, C., Lux, O., Marksteiner, U., Rahm, S., Weiler, F. et al. (2020a) Initial assessment of the performance of the first wind lidar in space on Aeolus. EPJ Web of Conferences. https://doi.org/10.1051/epjconf/202023701010

Reitebuch, O., Lemmerz, C., Nagel, E., Paffrath, U., Durand, Y., Endemann, M. et al. (2009) The airborne demonstrator for the direct-detection Doppler wind lidar ALADIN on ADM-Aeolus. Part I: instrument design and comparison to satellite instrument. *Journal of Atmospheric and Oceanic Technology*, 26, 2501–2515. Available from: https://doi.org/10.1175/2009JTECHA1309.1

Rennie, M.P., Isaksen, L., Weiler, F., de Kloe, J., Kanitz, T. & Reitebuch, O. (2021) The impact of Aeolus wind retrievals on ECMWF global weather forecasts. *Quarterly Journal of the Royal Meteorological Society*, 147, 3555–3586. Available from: https://doi.org/10.1002/qj.4142

Šavli, M., Pourret, V., Payan, C. & Mahfouf, J.-F. (2021) Sensitivity of Aeolus HLOS winds to temperature and pressure specification in the L2B processor. *Atmospheric Measurement Techniques*, 14, 4721–4736. Available from: https://doi.org/10.5194/amt-14-4721-2021

Stoffelen, A., Pailleux, J., Källén, E., Vaughan, J.M., Isaksen, L., Flamant, P. et al. (2005) The atmospheric dynamics Mission for global wind field measurement. *Bulletin of the American Meteorological Society*, 86(1), 73–87. Available from: https://doi.org/10.1175/BAMS-86-1-73

Straume-Lindner, A.G. (2018) 'Aeolus sensor and product description'. *Tech. Rep.*, European Space Agency–European Space Research and Technology Centre, The Netherlands. REF: AE-SU-ESA-GS-000. Available from: https://earth.esa.int/eogateway/documents/20142/37627/Aeolus-Sensor-and-Product-Description.pdf [Accessed 19 May 2021].

Wang, X. & Lei, T. (2014) GSI-based four-dimensional ensemble–variational (4DEnsVar) data assimilation: formulation and single-resolution experiments with real data for NCEP global forecast system. *Monthly Weather Review*, 142, 3303–3325. Available from: https://doi.org/10.1175/MWR-D-13-00303.1

Weiler, F., Rennie, M., Kanitz, T., Isaksen, L., Checa, E., Kloe, J.d. et al. (2021) Correction of wind bias for the lidar on-board Aeolus using telescope temperatures. *Atmospheric Measurement Techniques*, 14, 7167–7185. Available from: https://doi.org/10.5194/amt-14-7167-2021

How to cite this article: Liu, H., Garrett, K., Ide, K. & Hoffman, R.N. (2024) On the use of consistent bias corrections to enhance the impact of *Aeolus* Level-2B Rayleigh winds on National Oceanic and Atmospheric Administration global forecast skill. *Quarterly Journal of the Royal Meteorological Society*, 150(758), 355–372. Available from: https://doi.org/10.1002/qj.4600